



1 The importance of mineral determinations to PROFILE base

2 cation weathering release rates: A case study

3 Sophie Casetou-Gustafson¹, Cecilia Akselsson², Stephen Hillier^{1,3}, Bengt A. Olsson¹,

4

5 ¹Department of Ecology, Swedish University of Agricultural Sciences, (SLU), P.O. Box 7044, SE-750 07
6 Uppsala, Sweden

7 ²Department of Physical Geography and Ecosystem Science, Lund University, Sölvegatan 12, SE-223 62 Lund,
8 Sweden

9 ³The James Hutton Institute, Craigiebuckler, Aberdeen AB15 8QH, United Kingdom

10

11 *Correspondence to:* Sophie Casetou-Gustafson (Sophie.Casetou@slu.se)

12

13

14

15

16



17 Abstract

18 This study explored the influence of uncertainty in quantitative mineralogy on PROFILE base cation (Ca, Mg, K,
19 Na) weathering rates obtained using normative mineralogy compared to those obtained using measured
20 mineralogy, which was taken as a reference. Weathering rates were determined for two sites, one in Northern
21 (Flakaliden) and one in Southern (Asa) Sweden. At each site, 3–4 soil profiles were analyzed at 10 cm depth
22 intervals. Normative quantitative mineralogy was calculated from geochemical data and qualitative mineral data
23 with the “Analysis to Mineralogy” program (‘A2M’) using two sets of qualitative mineralogical data inputs to
24 A2M: A site-specific mineralogy determined from X-ray powder diffraction (XRPD) analyses, and regional
25 mineralogy, representing the assumed mineral identity and compositions for larger geographical areas in Sweden.
26 For the site-specific mineral input the precise elemental compositions of minerals were determined by microprobe
27 analysis, whereas for the regional mineralogy the compositions were as assumed in previous studies. A2M does
28 not provide a unique mineralogical solution and one thousand random mineralogical solutions were calculated by
29 A2M for each soil unit in order to include the full space of quantitative mineralogies in model outcome, all equally
30 possible. A corresponding number of PROFILE runs were made to estimate weathering rates. The contribution of
31 individual minerals to the release of base cations was also quantified by using a version of PROFILE which outputs
32 this detail. A discrepancy between weathering rates calculated from XRPD data (W_{XRPD}) and weathering rates
33 based on A2M (W_{A2M}) was only considered significant if the former was outside the full range of the latter.
34 Arithmetic means of W_{A2M} were generally in relatively close agreement with W_{XRPD} . The hypothesis that using
35 site-specific instead of regional mineralogy will improve the confidence in mineral data input to PROFILE was
36 supported for Flakaliden. However, at Asa, site-specific mineralogies reduced the discrepancy for Na between
37 W_{A2M} and W_{XRPD} but produced larger and significant discrepancies for K, Ca and Mg. For Ca and Mg the
38 differences between weathering rates based on different mineralogies could be explained by differences in the
39 content of some specific Ca- and Mg-bearing minerals, in particular amphibole, apatite, pyroxene and illite. It was
40 concluded that improving the precision in the content of those minerals would reduce weathering uncertainties.
41 High uncertainties in mineralogy, due for example to different A2M assumptions, had surprisingly low effect on
42 the weathering from Na- and K-bearing minerals. This can be explained by the fact that the weathering rate
43 constants for the minerals involved, e.g. K-feldspar and micas, are similar in PROFILE. Improving the description
44 of the dissolution rate kinetics of the plagioclase mineral group as well as major K-bearing minerals (K-feldspars
45 and micas) should be of particular importance to future weathering estimates.
46

47



48 **Definitions and abbreviations**

49

50 Mineralogy = the identity (specific mineral or mineral group) and stoichiometry (specific mineral chemical
51 composition) of minerals that are present at a certain geographic unit, a particular site (*site-specific mineralogy*)
52 or a larger geographic province (*regional mineralogy*)

53 Quantitative mineralogy = the quantitative information (wt.%) on the abundance of specific minerals in
54 the soil.

55 **Abbreviations:**

56 M_{XRPD} = quantitative mineralogy based on XRPD (amount) and electron microprobe analysis (composition)

57 $M_{A2M-reg}$ = quantitative mineralogy calculated with the A2M model and using regional mineralogy

58 $M_{A2M-site}$ = quantitative mineralogy calculated with the A2M model and using site-specific mineralogy

59 W_{XRPD} = weathering rate based on quantitative mineralogy determined by XRPD and electron microprobe analysis

60 W_{A2M} = weathering rate based on quantitative mineralogy determined by the A2M model (unspecific mineralogy)

61 $W_{A2M-reg}$ = weathering rate based on quantitative mineralogy determined by the A2M model, and assuming regional
62 mineralogy.

63 $W_{A2M-site}$ = weathering rate based on quantitative mineralogy determined by the A2M model and assuming site-
64 specific mineralogy.

65

66

67



68 1. Introduction

69 The dissolution of minerals during weathering represents, together with deposition, the most important long-term
70 supply of base cations for plant growth as well as acting as a buffer against soil and water acidification. Quantifying
71 weathering rates is therefore of key importance to guide modern forestry demands on biomass removal by helping
72 to identify threshold levels of sustainable base cation removal from soils and waters. With the introduction of the
73 harvest of forest biomass for energy production that includes whole tree harvest and stump extraction, about 2–3
74 times more nutrients are exported from the forest compared to stem-only harvest. As a result, issues of acidification
75 and base cation supply are exacerbated and the sustainability of this practice is questioned (Röser, 2008; de Jong
76 et al. 2017). Regional nutrient balance calculations for Sweden have indicated that net losses of base cations from
77 forest soils can occur in stem-only harvest scenarios, and this trend was substantially exacerbated and became
78 more frequent in whole-tree harvesting scenarios, largely due to low weathering rates (Sverdrup and Rosén, 1998;
79 Akselsson et al., 2007a,b). The same effect occurred both under current and projected future climate conditions
80 (Akselsson et al., 2016).

81 The weathering rates included in these nutrient balance calculations are in most cases based on the PROFILE
82 model. This model is the most used mechanistic tool to calculate steady state chemical weathering at the interface
83 of soil minerals and their surrounding liquid solution (Sverdrup, 1996), and has been widely applied in Europe
84 and the US during the last several decades or more of weathering research (Olsson et al., 1993; Langan et al., 1995;
85 Kolka et al., 1996; Starr et al., 1998; Sverdrup and Rosén, 1998; Koseva et al., 2010; Whitfield et al., 2006;
86 Akselsson et al., 2007a; Stendahl et al., 2013). In a few cases nutrient balance calculations have also been based
87 on the depletion method (Olsson et al., 1993).

88 Reliable weathering rate estimates are crucial for the accuracy of future nutrient budget calculations (Futter et al.,
89 2012). Regarding the accuracy of the PROFILE model, the importance of high accuracy in physical input
90 parameters for the modelled weathering rate outputs has been highlighted by Hodson et al. (1996) and Jönsson et
91 al. (1995). Among these parameters Hodson et al. (1996) noted that the weathering response of the entire soil
92 profile depends critically on its mineralogy. However, little attention has been given to the influence of modelled
93 versus directly measured mineralogical input data on calculated base cation release rates.

94 The most widely used method for direct quantitative mineralogical analysis of soil samples is X-ray powder
95 diffraction, and the accuracy that can be achieved has been demonstrated in round robin tests most notably the
96 Reynolds Cup (McCarty, 2002; Kleeberg, 2005; Omotoso et al., 2006, Raven and Self, 2017). Casetou-Gustafson
97 et al. (2018) made some independent assessment of the accuracy of their own XRPD data by geochemical cross
98 validation (i.e. the mineral budgeting approach of Andrist-Rangel et al., 2006). Nonetheless, we should stress that
99 like all analytical methods the determined weight fractions of minerals identified in a soil sample by XRPD will
100 have an associated uncertainty, and additionally minerals present in minor amounts, nominally < 1% by weight,
101 may fall below the lower limit of detection of the XRPD method.

102 Due mainly to the relative ease of measurement and consequent ready availability of total element geochemical
103 data on soils, indirect methods of determining quantitative soil mineralogy, such as so called ‘normative’
104 geochemical calculations have been widely used to generate mineralogical data for use in the PROFILE model.
105 One such method is the normative “Analysis to Mineralogy” (A2M) program (Posch and Kurz, 2007) that has



106 commonly been used in PROFILE applications (Stendahl et al. 2013; Zanchi et al. 2014, this issue; Yu et al. 2016;
107 2018; Kronnäs et al., 2019). Based on a quantitative geochemical analysis of a soil sample, typically expressed in
108 weight percent oxides, and also on some assessment of the available minerals in the soil sample (minerals present)
109 and their stoichiometry (chemical compositions), A2M calculates all possible mineralogical compositions. The
110 A2M output for a given soil sample input has multiple solutions and can be described as a multidimensional
111 mineralogical solution space. This necessitates a choice when using A2M output in applications such as weathering
112 rate studies, the convention for which has been to use the geometric mean mineralogical compositions e.g. Stendahl
113 et al. 2013. Casetou-Gustafson et al. (2018) compared the output of A2M with directly determined XRPD
114 mineralogies at two sites, applying A2M in two different ways. In the first case the information on available
115 minerals in the model input was obtained from direct XRPD mineral identifications and information on mineral
116 stoichiometry from direct microprobe analysis of the minerals at the specific site (hereafter denoted "site-
117 specific"). In the second case the mineral stoichiometry and mineral identity were both assumed based on an expert
118 assessment of the probable mineralogy at the regional scale as given by Warfvinge and Sverdrup (1995), hereafter
119 denoted "regional". Casetou-Gustafson et al. (2018) concluded that using A2M in combination with regional input
120 data yielded results with large deviations from directly (XRPD) measured quantitative mineralogy, particularly for
121 two of the major minerals, K-feldspar and dioctahedral mica. When site-specific mineralogical input data was
122 used, measured and modeled quantitative mineralogy showed a better correspondence for most minerals. For a
123 specific mineral and a specific site, however, the bias in determination of quantitative mineralogy might be
124 significant depending on the accuracy of input data to A2M, i.e. total geochemistry and/or mineral stoichiometry
125 (Casetou-Gustafson et al., 2018). Errors like these in mineralogical input data might be assumed to affect the
126 calculated weathering for different base cations significantly.

127 In the present study, we used the different mineralogical data from Casetou-Gustafson et al. (2018) to model
128 weathering rates of soils with the PROFILE model. Rates calculated based on measured mineral abundances using
129 quantitative XRPD in combination with measured elemental compositions are taken as 'reference' weathering
130 rates to which other rates are compared. Samples for this study were collected from podzolised till soils from 8
131 soil profiles at two forest sites in northern and southern Sweden, respectively.

132 The primary objective of this study was to describe and quantify the effect of differences in mineralogy input on
133 PROFILE weathering rates, leaving all other input parameters of the PROFILE model constant to isolate the effects
134 of mineral stoichiometry and abundance. A first specific aim was to determine the uncertainties in weathering rates
135 caused by uncertainties in normative quantitative mineralogy. This was approached by comparing PROFILE runs
136 using modeled mineralogies based on the presence of minerals of a specific site or a larger geographic region (i.e.
137 site-specific and regional mineralogy) with PROFILE runs using the directly measured mineralogy. The latter was
138 assumed to represent the 'true' mineralogy at each site. This comparison of PROFILE weathering rates, based on
139 XRPD versus A2M mineralogy, was done using 1000 random solutions per sample from the entire
140 multidimensional A2M solution space. In the following, weathering rates calculated by PROFILE based on XRPD
141 and A2M mineralogies are denoted W_{XRPD} and W_{A2M} , respectively.

142 A second specific aim was to investigate how the over- or underestimation of W_{A2M} in relation to W_{XRPD} mirrors
143 the over- or underestimation of mineral contents estimated with A2M.



144 The following hypotheses were made:
145 (1) PROFILE weathering rates obtained with site-specific mineralogical data are more similar to the reference
146 weathering rates than PROFILE runs obtained with regional mineralogical input data
147 (2) Over- and underestimations of weathering rates of different base cations by the PROFILE model can be
148 explained by over- and underestimations of mineral contents of a few specific minerals.

149

150 2. Materials and methods

151 2.1 Study sites

152 Two experimental forest sites, Asa in southern, and Flakaliden in northern Sweden, were used for the study (Table
153 1). Both sites have Norway spruce (*Picea abies* (L.) Karst) stands of uniform age, but differ in climate. Flakaliden
154 is located in the boreal zone with long cold winters, whereas Asa is located in the hemiboreal zone. The soils have
155 similar texture (Sandy loamy till), soil types (Spodosols) and moisture conditions. According to the geographical
156 distribution of mineralogy types in Sweden the sites belong to different regions (Warfvinge and Sverdrup, 1995).
157 The experiments, which started in 1986, aimed at investigating the effects of optimized water and nutrient supply
158 on tree growth and carbon cycling in Norway spruce forests (Linder 1995, Albaugh et al. 2009). The sites are
159 incorporated in the Swedish Infrastructure for EcosystemScience (SITES).

160 2.2 Soil sampling and stoniness determination

161 Soil sampling was performed in October 2013 and March 2014 in the border zone of four plots each of the sites.
162 Plots selected for sampling were untreated control plots (K1 and K4 at Asa, 10B and 14B at Flakaliden) and
163 fertilized 'F' plots (F3, F4 at Asa, 15A, 11B at Flakaliden). A rotary drill was used in order to extract one intact
164 soil core per plot (17 cm inner diameter) expect for plot K4, F3 and F4 at the Asa site. A 1 x 1m soil pit was
165 excavated at each of the three latter plots due to inaccessible terrain for forest machinery. The maximum mineral
166 soil depth varied between 70–90 cm in Flakaliden and 90–100 cm in Asa.

167

168 The volume of stones and boulders was determined with the penetration method by Viro (1952), and by applying
169 penetration data to the functions by Stendahl et al. (2009). A metal rod was penetrated at 16 points per plot into
170 the soil until the underground was not possible to penetrate any further, or to the depth 30 cm. There was a higher
171 average stoniness at Flakaliden than Asa (39 vol-% compared to 29 vol-% in Asa) that could partially explain the
172 lower maximum sampling depth at Flakaliden.

173 2.3 Sample preparation

174 Soils samples for chemical analyses were taken at 10 cm depth intervals in the mineral soil. Prior to analysis all
175 soil samples were dried at 30–40 °C and sieved at 2 mm mesh. Soil chemical analyses were performed on the fine
176 earth fraction (<2mm).



177 2.4 Analysis of geochemistry, total carbon and soil texture

178 Total carbon was determined using a LECO elemental analyzer according to ISO 10694. Analysis of total
179 geochemical composition, conducted by ALS Scandinavia AB, was made by inductively coupled plasma
180 spectrometry (ICP-MS). Prior to analyses, the samples were ignited at 1000° C to oxidize organic matter and
181 grinded with an agate mortar. Particle size distribution was analyzed by wet sieving and sedimentation (Pipette
182 method) in accordance with ISO 11277. More details about the analytical procedure was given by Casetou-
183 Gustafson et al. (2018).

184 2.5 Determination of quantitative mineralogy

185 A detailed description of methods used to quantify mineralogy of the samples were given by Casetou et al.
186 (2018), and are described in brief below.

187 2.5.1 Measured mineralogy

188 Quantitative soil mineralogy was determined with the X-ray powder diffraction technique, XRPD (M_{XRPD}) (Hillier
189 1999, 2003). Preparation of samples for determination of XRPD patterns was made from spraying and drying
190 slurries of micronized soil samples (<2 mm) in ethanol. Quantitative mineralogical analysis of the diffraction data
191 was performed using a full pattern fitting approach (Omotoso et al., 2006). In the fitting process, the measured
192 diffraction pattern is modelled as a weighted sum of previously recorded and carefully verified standard reference
193 patterns of the prior identified mineral components. The chemical composition of the various minerals present in
194 the soils was determined by electron microprobe analysis (EMPA).

195 2.5.2 Calculated mineralogy

196 The A2M program (Posch and Kurz, 2007) was used to calculate quantitative mineralogical composition (M_{A2M})
197 from geochemical data. Based on a set of pre-determined data on mineral identity and stoichiometry, the model
198 outcome is a range of equally possible mineralogical compositions. The multidimensional structure of this
199 normative mineralogy model is a consequence of the number of minerals being larger than the number of analysed
200 elements, where a specific element can often be contained in several different minerals. A system of linear
201 equations is used to construct an M-N dimensional solution space (Dimension M= Number of minerals, Dimension
202 N=number of oxides). In this study we used one thousand solutions to cover the range of possible quantitative
203 mineralogies that may occur at a specific site.

204

205 A2M was used to calculate 1000 quantitative mineralogies each for two different sets of mineral identity and
206 element stoichiometry, $M_{A2M-reg}$ (regional) and $M_{A2M-site}$ (site-specific). Regional mineralogy refers to the mineral
207 identity and stoichiometry for the four major mineralogical provinces in Sweden suggested by Warfvinge and
208 Sverdrup (1995), of which Asa and Flakaliden belong to different regions. Site-specific mineralogy refers to the
209 measured mineral identity and stoichiometry determined by the XRPD and electron microprobe analyses of the
210 two sites (Casetou-Gustafson et al., 2018).



211 2.6. Estimation of weathering rates with PROFILE

212 2.6.1 PROFILE model description

213 The biogeochemical PROFILE model can be used to study the steady state weathering (i.e. stoichiometric mineral
214 dissolution) of soil profiles, as weathering is known to be primarily determined by the physical soil properties at
215 the interface of wetted mineral surfaces and the soil solution. PROFILE is a multilayer model, thus, for each soil
216 layer, parameters are specified based on field measurements and estimation methods (Warfvinge and Sverdrup,
217 1995). Furthermore, isotropic, well mixed soil solution conditions are assumed to prevail in each layer as well as
218 surface limited dissolution in line with early views by Aagard and Helgeson (1982) and Cou and Wollast (1985)
219 (Sverdrup, 1996). Based on these major assumptions, PROFILE calculates chemical weathering rates from a series
220 of kinetic reactions that are described by laboratory determined dissolution rate coefficients and soil solution
221 equilibria (i.e. transition state theory) (Sverdrup and Warfvinge, 1993). The PROFILE version (September 2018)
222 that was used in this study is coded to produce information on the weathering contribution of specific minerals,
223 which allowed us to test our second hypothesis. This version is based on the weathering rates of 15 minerals. Of
224 these, apatite, pyroxene, illite, dolomite and calcite were not found at the two study sites according to XRPD data
225 (Table S1).

226 2.6.2 PROFILE parameter estimation

227 The only parameter that was changed between different PROFILE runs was the quantitative mineralogy for each
228 soil layer, as described above. Hence, PROFILE estimated weathering rates (W) based on measured mineralogy
229 (W_{XRPD}), and the two versions of A2M calculated mineralogy, regional ($W_{A2M-reg}$), and site-specific ($W_{A2M-site}$). In
230 the regional mineralogy, plagioclase is assumed to occur as pure anorthite and pure albite for simplification as has
231 been used in previous studies (Stendahl et al., 2013; Zanchi et al., 2014). This simplification was done in order to
232 avoid having a number of minerals containing different amount of Ca and Na, as a result of plagioclase forming a
233 continuous solid solution series, since it would not affect the weathering rates.

234

235 The physical soil layer specific parameters, that were kept constant between different profile runs, were exposed
236 mineral surface area, stoniness, soil bulk density and soil moisture (Table 2). Exposed mineral surface area was
237 estimated from soil bulk density and texture analyses in combination with an algorithm specified in Warfvinge
238 and Sverdrup (1995). The volumetric field soil water content in Flakaliden and Asa was estimated to be $0.25 \text{ m}^3 \text{ m}^{-3}$
239 according to the moisture classification scheme described in Warfvinge and Sverdrup (1995). It was used to
240 describe the volumetric water content for each soil pit.

241

242 Another group of parameters kept constant was chemical soil layer specific parameters. Aluminum solubility
243 coefficient needed for solution equilibrium reactions, defined as $\log\{\text{Al}^{3+}\} + 3\text{pH}$, was estimated applying a
244 function developed from previously published data (Simonsson and Berggren, 1998) on our own total carbon and
245 oxalate extractable aluminum measurements. The function is based on the finding that the Al solubility in the
246 upper B-horizon of Podzols is closely related to the molar ratio of aluminum to carbon in pyrophosphate extracts,
247 and that below the threshold value of 0.1, Al solubility increases with the Al_p/C_p ratio (Simonsson and Berggren,
248 1998). Thus, a function was developed for application to our own measurements of Al_{ox} and C_{tot} based on the
249 assumption that it is possible to use the $\text{Al}_{ox}/\text{C}_{tot}$ ratio instead of the Al_p/C_p ratio. Data on soil solution DOC were



250 available from lysimeters installed at 50 cm depth for plot K4 and K1 in Asa and 10B and 14B in Flakaliden, and
251 these values were also applied to soil depths below 50 cm (H. Grip, unpublished data). The E-horizon (0–10 cm
252 at Flakaliden) and A-horizon (0–10 cm at Asa) were characterized by higher DOC values based on previous
253 findings (Fröberg et al., 2013) and the classification scheme of DOC in Warfvinge and Sverdrup (1995). Partial
254 CO₂ pressure values in the soil were taken from the default estimate of Warfvinge and Sverdrup (1995).

255

256 Other site-specific parameters that were kept constant between PROFILE runs were evapotranspiration,
257 temperature, atmospheric deposition, precipitation, runoff and nutrient uptake. An estimate of the average
258 evaporation per site was derived from annual averages of precipitation and runoff data using a general water
259 balance equation. Deposition data from two sites of the Swedish ICP Integrated Monitoring catchments, Aneboda
260 (for Asa) and Gammtratten (for Flakaliden) (Löfgren et al., 2011) were used to calculate the total deposition. The
261 canopy budget method of Staelens et al. (2008) was applied as in Zetterberg et al. (2014) for Ca²⁺, Mg²⁺, K⁺, Na⁺.
262 The canopy budget model is commonly used for elements that are prone to canopy leaching (Ca²⁺, Mg²⁺, K⁺, Na⁺,
263 SO₄²⁻) or canopy uptake (NH₄⁺, NO₃⁻) and calculates the total deposition (TD) as the sum of dry deposition (DD)
264 and wet deposition (WD). Wet deposition was estimated based on the contribution of dry deposition to bulk
265 deposition, both for base cations and anions, using dry deposition factors from Karlsson et al. (2012). Base cation
266 and nitrogen accumulation rate in above-ground tree biomass (i.e. bark, stemwood, living and dead branches,
267 needles) was estimated as the average accumulation rate over a 100 years rotation length in Flakaliden compared
268 to a 73 years rotation length in Asa. These calculations were based on Heureka simulations using the StandWise
269 application (Wikström et al., 2011) for biomass estimates in combination with measured nutrient concentrations
270 in above-ground biomass (S. Linder unpubl. data).

271 **2.7 A definition of significant discrepancies between W_{A2M} and W_{XRPD}**

272 A consequence of the mathematical structure of the A2M program is that the space of possible quantitative
273 mineralogies in the end produces an uncertainty range of weathering estimates, but in a different sense than the
274 uncertainty caused by e.g. uncertainties in chemical analyses, because all mineralogies produced within this range
275 are equally likely. Thus, here we define a significant discrepancy between W_{XRPD} and W_{A2M} to occur when the
276 former is outside the range of the latter, as illustrated in Fig. 1a. The opposite case is a non-significant discrepancy,
277 when the weathering rates based on XPRD are contained in the weathering range based on A2M (Figure 1b).

278

279 The uncertainty range of W_{A2M} can potentially be reduced by reducing uncertainties in analyses of soil
280 geochemistry but most particularly by definitions of available minerals and their stoichiometry. Furthermore, some
281 discrepancies between W_{XRPD} and W_{A2M} might also arise due to limitations of the XRPD method, particularly
282 when minerals occur near or below the detection limit.

283 **2.8 Statistical analyses**

284 In order to quantify the effect of mineralogy on PROFILE weathering rates two statistical measures were used to
285 describe the discrepancies between W_{XRPD} and W_{A2M}. Firstly, root mean square errors (RMSE) of the differences
286 between W_{XRPD} and the arithmetic mean of weathering rates based on regional and site-specific mineralogy, i.e.,
287 W_{A2M-reg} and W_{A2M-site}, were calculated:



288
$$\text{RMSE} = \sqrt{\frac{1}{n} \sum_{i=1}^n (\text{W}_{\text{XRPD}} - \text{W}_{\text{A2M}})^2} \quad \text{Eq. (1)}$$

289 RMSE's were calculated individually for each element, soil layer and soil profile for two data sets. An RMSE
290 expressing the error of the aggregated, total weathering rates in the 0–50 cm soil horizon was calculated to test our
291 first hypothesis (RMSE of total weathering). In addition, an RMSE expressing the errors originating from
292 discrepancies between W_{XRPD} and W_{A2M} for individual minerals was also calculated (RMSE of weathering by
293 mineral). In the latter case, sums of RMSE's by mineral were calculated for each element and soil profile in analogy
294 with the summing up of weathering rates for the whole 0–50 cm soil profile.

295

296 Secondly, relative discrepancies (i.e. average percentage of over- or underestimation of W_{A2M} compared to W_{XRPD})
297 were calculated as the absolute discrepancy divided by the measured value.

298

299
$$\text{Relative error} = \left(\frac{(\text{W}_{\text{A2M}})_i - \text{W}_{\text{XRPD}})_i}{\text{W}_{\text{XRPD}}_i} \right) * 100 \quad \text{Eq. (2)}$$

300

301 Relative errors were calculated for each site by comparing the average sum of W_{A2M} in the upper mineral soil (0–
302 50 cm) with the sum of W_{XRPD} in the upper mineral soil.

303 Statistical plotting of results was performed using R (version 3.3.0) (R Core Team, 2016) and Excel 2016.

304 **3. Results**

305 **3.1 Weathering rates based on XRPD mineralogy**

306 Weathering estimates with PROFILE are hereafter presented as the sum of weathering rates in the 0–50 cm soil
307 horizon, since this soil depth is commonly used in weathering rate studies. Information on individual, and deeper
308 soil layers (50–100 cm) is given in Table S2.

309

310 Weathering rates of the base cations based on quantitative XRPD mineralogy (W_{XRPD}), the reference weathering
311 rates, were ranked in the same order at both sites, i.e., Na>Ca>K>Mg (Table S2). On average, weathering rates of
312 Na, Ca, K and Mg at Asa were 17.7, 8.4, 5.6 and 3.6 $\text{mmol}_c \text{ m}^{-2} \text{ yr}^{-1}$, respectively. Corresponding figures for
313 Flakaliden were of similar magnitude, i.e., 14.8, 9.8, 5.7 and 5.6 $\text{mmol}_c \text{ m}^{-2} \text{ yr}^{-1}$. The variation in weathering rates
314 between soil profiles was smaller at Asa than at Flakaliden, as the standard deviation in relation to the means for
315 different elements ranged between 0.2–2.3 at Asa, and 2.0–5.7 at Flakaliden (Table S2).

316

317 **3.2 Comparison between weathering rates based on XRPD and A2M mineralogy**

318 At Flakaliden, $\text{W}_{\text{A2M-site}}$ was generally in closer agreement with W_{XRPD} than $\text{W}_{\text{A2M-reg}}$ (Fig. 2b), in line with the first
319 hypothesis. The discrepancies between W_{XRPD} and W_{A2M} were small and non-significant for Mg regardless of the
320 mineralogy input used in A2M, although the estimated discrepancies were reduced when site-specific mineralogy
321 was used. The use of regional mineralogy in A2M underestimated K release rates compared to W_{XRPD} , and the
322 discrepancy was significant. Using site-specific mineralogy resulted in smaller and non-significant discrepancy
323 for K release rates. A similar response to different mineralogies was revealed for Ca, although the result varied
324 more among soil profiles. In contrast to K and Ca, the release of Na was overestimated by both $\text{W}_{\text{A2M-site}}$ and $\text{W}_{\text{A2M-reg}}$.



325 $W_{A2M-reg}$ compared to W_{XRPD} . The discrepancies were significant regardless of the mineralogy input used in A2M,
326 although using site-specific mineralogy slightly reduced the discrepancy. The generally closer agreement between
327 $W_{A2M-site}$ and W_{XRPD} than $W_{A2M-reg}$ at Flakaliden was also indicated by the lower RMSEs of total weathering for all
328 base cations when site-specific mineralogy was used (Fig. 3a). Relative RMSE were below 20 % for $W_{A2M-reg}$, but
329 below 10 % for $W_{A2M-site}$. However, RMSE for Na was only slightly smaller for $W_{A2M-site}$ than $W_{A2M-reg}$ (16 % for
330 $W_{A2M-site}$).

331

332 PROFILE weathering rates for Asa revealed a different pattern compared to Flakaliden, and the results for Ca, Mg
333 and K were contradictory to hypothesis one. $W_{A2M-reg}$ was in close agreement with W_{XRPD} for K, Ca and Mg, and
334 the small discrepancies were non-significant (Fig. 2a). However, $W_{A2M-reg}$ for Na was consistently overestimated
335 compared to W_{XRPD} and the discrepancies were significant. Using site-specific mineralogy improved the fit
336 between W_{XRPD} and W_{A2M} for Na, but had rather the opposite effect on the other base cations at this site. For K,
337 Ca and Mg, $W_{A2M-site}$ overestimated weathering rates, and resulted in significant discrepancies, and larger RMSE,
338 whereas the discrepancies for Na were reduced and non-significant (Fig. 3a). At Asa, the highest relative RMSEs
339 of total weathering occurred for Ca and Mg with $W_{A2M-site}$ (> 30 %) (Fig. 3a). Large standard deviations were due
340 to a single soil profile, F4. The better consistency with $W_{A2M-reg}$ was indicated by RMSE below 10 % for Ca and
341 Mg, and that RMSE for Mg was half of the error with $W_{A2M-site}$. Only for Na, RMSE was lower for $W_{A2M-site}$ than
342 with $W_{A2M-reg}$.

343

344 A complementary illustration of the relationships between weathering rates based on XRPD and A2M is shown in
345 Fig. 4 and provided as Tables S3 and S4, which includes all data from individual soil layers 0–50 cm. A general
346 picture is that $W_{A2M-site}$ was less dispersed along the 1:1-line than $W_{A2M-reg}$, in particular for Flakaliden. On the
347 other hand, for weathering rates in the lower range (< 5 mmol_c m⁻² yr⁻¹) site-specific mineralogy tended to generate
348 both over- and underestimated weathering rates. In most soil profiles, deviations from the 1:1-line were frequent
349 in soil layers below 20 cm. For Na under- and overestimations occurred in the whole range of weathering
350 estimates,

351 3.3 Mineral-specific contribution to weathering rates

352 In spite of its intermediate dissolution rate plagioclase was, due to its abundance, the most important Na-bearing
353 mineral determined in this study (Table 3 and Fig. 5). Plagioclase is a variable group of minerals with different
354 stoichiometric proportions of Ca and Na, from the purely sodic albite on the one hand to the purely calcic anorthite
355 on the other hand (Table S5) as well as with intermediate compositions (Table S6). For simplicity, they will be
356 referred to in this study as sodic and calcic plagioclase. Based on the same quantitative mineralogy (i.e. same
357 elemental compositions and identity of minerals), W_{XRPD} and $W_{A2M-site}$ gave strong weight to both calcic and sodic
358 plagioclase in estimating Na release rates, but $W_{A2M-site}$ gave stronger weight to calcic versus sodic plagioclase at
359 Asa, and vice-versa at Flakaliden (Fig. 5). In spite of these differences, the resultant release rates of Na according
360 to $W_{A2M-site}$ and W_{XRPD} were rather similar (Fig. 5).

361

362 Total Na release rates of $W_{A2M-reg}$ compared to W_{XRPD} were moderately overestimated. The relative RMSE of
363 weathering by specific Na-containing minerals were of more similar magnitude for Na at Flakaliden compared to



364 Asa (Fig. 3b). However, the standard deviations of RMSE were relatively large at Flakaliden, due to large RMSE
365 for albite in one specific soil profile (11B) (Table S7). Contrary to relative RMSE of total weathering, the relative
366 RMSE of weathering by specific minerals was lower for Na at Asa with regional than site-specific mineralogy.
367
368 According to W_{XRPD} , calcic plagioclase weathering was the most important source to Ca release at Flakaliden, and
369 the second most important source at Asa after epidote (Fig. 5). As for Na, $W_{A2M-site}$ gave stronger weight to calcic
370 plagioclase than W_{XRPD} at Asa. It was the other way around for $W_{A2M-site}$ at Flakaliden and the regional mineralogy
371 (i.e. W_{XRPD} stronger weight to calcic plagioclase than $W_{A2M-site}$). Another important Ca source in weathering
372 estimates based on A2M was apatite. This mineral was not detected in the XRPD analyses, but was included in
373 both A2M mineralogies as a necessary means to allocate measured total phosphorus content to a specific mineral
374 (Casetou-Gustafson et al. 2018).
375
376 Similar to Na, relative RMSE of weathering by Ca-containing minerals were several magnitudes larger than RMSE
377 of the total weathering of Ca. In other words, although an overall similar weathering rates might be generated by
378 the PROFILE model based on different quantitative mineralogies, the underlying contributions from different
379 minerals can be markedly different. At Flakaliden, the mean relative RMSE by specific minerals were larger for
380 regional than site-specific mineralogy at Flakaliden (Fig. 3b). However, the difference was not significant since
381 the standard deviations were high, probably due to larger RMSE for Ca-bearing minerals in soil profile 11B (Table
382 S7).
383
384 A general picture of the mineral contribution to Mg release is that W_{XRPD} placed most weight to amphibole whereas
385 in W_{A2M} Mg release was more equally distributed among other minerals, notably hydrobiotite, trioctahedral mica
386 and vermiculite. At Asa, and to an even larger extent at Flakaliden, Mg release by A2M mineralogies was
387 determined by a higher contribution of minerals with high dissolution rates (Fig. 5 and Table 3) (i.e. In $W_{A2M-site}$,
388 hydrobiotite and trioctahedral mica; In $W_{A2M-reg}$, muscovite and vermiculite at Asa and biotite and illite at
389 Flakaliden). At Asa, less weight was given to amphibole by $W_{A2M-site}$ compared to W_{XRPD} . At Flakaliden, the $W_{A2M-
390 site}$ was close W_{XRPD} in spite of the very different allocations of weathering rates to different minerals. The
391 underestimation of Mg release by $W_{A2M-reg}$ was largely explained by the lower weight given to amphibole in both
392 A2M scenarios (Fig. 5). However, A2M gave larger weight to other minerals. The sums of RMSEs of weathering
393 from specific Mg-bearing minerals were much larger for regional than site-specific mineralogy at Flakaliden and
394 reached a maximum value of 156 %. A contributing factor were generally larger RMSE for the mineral
395 contribution of amphibole to Mg weathering and the fact that pyroxene contributed to the RMSEs of the total
396 weathering of Mg. Furthermore, a large standard deviation for the sum of RMSE of specific minerals (Fig. 3b)
397 was caused by soil profile 11B where more weight was placed on amphibole and biotite in contributing to Mg
398 weathering (Table S7). The two A2M mineralogies resulted in the same RMSEs for Mg-bearing minerals at Asa
399 (Fig. 3b).
400
401 Potassium release rates were largely dominated by K-Feldspar weathering in both W_{XRPD} and $W_{A2M-site}$. However,
402 K release by $W_{A2M-reg}$ (Fig. 5) were largely determined by micas at both sites. Together with Mg, these elements
403 had also the lowest weathering rates, indicating that differences between $W_{A2M-reg}$ and W_{XRPD} in relative terms were



404 not correlated with the magnitude of weathering. Unlike the other base cations, relative RMSE of K-bearing
405 minerals were lower at both sites when site-specific mineralogy was used instead of regional (Fig. 3b), and the
406 mineral specific RMSEs were also of similar magnitude as the RMSE of the total weathering (Fig. 3a). $W_{A2M\text{-site}}$ of
407 K (Fig. 3b), were not several magnitudes larger than RMSE of the total weathering (Fig. 3a). The largest relative
408 RMSEs of K-containing minerals were reached by $W_{A2M\text{-reg}}$ at Flakaliden in soil profile 11B, indicated by the high
409 standard deviation.

410 **4. Discussion**

411 **4.1 General range of weathering rates in relation to expectations from other sensitivity studies, and the**
412 **range of discrepancies between W_{XRPD} and $WA2M$**

413 To our knowledge, the present study is the first to have examined the sensitivity of the PROFILE model on real
414 case study differences of directly measured mineralogy versus indirectly determined normative mineralogy.
415 However, a few systematic studies have been made previously to test the influence of mineralogy inputs, amongst
416 other input parameters, to PROFILE weathering rates. Jönsson et al. (1995) concluded that uncertainty in
417 quantitative mineralogy could account for a variation from the best weathering estimate of about 20 %, and that
418 variations in soil physical and chemical parameters could be more important. The sensitivity analysis of Jönsson
419 et al. (1995) was made by a Monte Carlo simulation where mineralogical inputs were varied by ± 20 % of abundant
420 minerals, and up to ± 100 % of minor minerals. Shortly after, Hodson et al. (1996) examined the sensitivity of the
421 PROFILE model with respect to the sensitivity of weathering of specific minerals and concluded that large
422 uncertainties in particular in soil mineralogy, moisture, bulk density, temperature and surface area determinations
423 will have a larger effect on weathering rates than was reported by Jönsson et al. (1995).

424 Compared with the sensitivity analyses by Jönsson et al. (1995), the range of uncertainty in dominating mineral
425 inputs used in the present study was of similar order of magnitude. For this study we used the XRPD measured
426 (M_{XRPD}) and A2M estimated mineralogies (M_{A2M}) determined by Casetou-Gustafson et al. (2018). For example,
427 they concluded that $M_{A2M\text{-reg}}$ produced a low relative RMSE of total plagioclase (7 – 11 %) but higher relative
428 RMSE for less abundant minerals, such as dioctahedral mica (90 – 106 %). They also showed that when regional
429 mineral identity and assumed stoichiometry was replaced by site-specific mineralogy ($M_{A2M\text{-site}}$), the bias in
430 quantitative mineralogy was reduced.

431 Thus, given this bias in quantitative mineralogy input to PROFILE, discrepancies of W_{A2M} from W_{XRPD} at our
432 study sites should have been on the order of 20 % or less, and site-specific mineralogy inputs should produce
433 weathering rates with lesser discrepancies than regional mineralogy. The result of this study was in agreement
434 with this expectation for all elements at Flakaliden but only for Na at Asa. The different quantitative mineralogies
435 resulted in discrepancies between W_{A2M} and W_{XRPD} that differed with site (Fig. 3a, 5).

436 **4.2 Is $W_{A2M\text{-site}}$ more consistent than $W_{A2M\text{-reg}}$?**

437 Our first hypothesis, that using site-specific mineralogy in the PROFILE model compared to regional mineralogy,
438 should result in weathering rates closer to XRPD-based mineralogy, and thus be more consistent, was generally
439 supported for Flakaliden, but only for Na at Asa. This result was revealed from both the occurrence of significant
440 discrepancies as well as the RMSE of the total weathering rates. Thus, the results did not support our first



441 hypothesis in a consistent way. The possible reasons for this outcome are discussed below, based on the analysis
442 of how different minerals contributed to the overall weathering rates.

**443 4.3 How are discrepancies between W_{A2M} and W_{XRPD} correlated to bias in determinations of quantitative
444 mineralogy**

445 The version of the PROFILE model used in this study allowed a close examination of the per element weathering
446 rate contributions obtained from different minerals that provide some insight into the causes to the total W_{A2M}
447 discrepancies.

448 4.3.1 Sodium release rates

449 A biased determination of mineralogy may not necessarily result in a corresponding bias of PROFILE weathering
450 estimates if the discrepancies are cancelling each other out, and if dissolution rates of the different minerals are
451 rather similar. This was probably the case for Na. At both study sites and for both W_{XRPD} and W_{A2M} , Na release
452 rates were largest for plagioclase minerals. The Na release from $W_{A2M\text{-site}}$ and $W_{A2M\text{-reg}}$ were close to W_{XRPD} at both
453 study sites (i.e. all weathering rates were in the range of 17-19 mmol_c m⁻² yr⁻¹) in spite of that $W_{A2M\text{-site}}$ placed
454 more weight to calcic plagioclase and $W_{A2M\text{-reg}}$ more weight to albitic plagioclase (Fig.5). Contrary to our second
455 hypothesis, the relatively high precision in total release rates (i.e. <10%; Fig. 3a) of Na was not correlated to the
456 actual low precision in mineral contribution to the total Na release rates (i.e. >30%; Fig. 3b). The latter can be
457 explained by the fact that in PROFILE all types of plagioclase have the same dissolution rate coefficients (Table
458 3). Due to this, and in combination with the fact that plagioclase type minerals are a major source for Na, the
459 mineralogical uncertainty in estimating Na release rates with PROFILE was relatively low in this study (i.e. <20
460 %). In context, however, we note that it is generally accepted that under natural conditions different plagioclase
461 minerals weather at different rates, (Allen and Hajek, 1989, Blum and Stillings, 1995).

462 4.3.2 Calcium release rates

463 According to W_{XRPD} and W_{A2M} , a key mineral for Ca release rates was calcic plagioclase at Flakaliden and epidote
464 at Asa. In line with our second hypothesis, the overestimation of calcic plagioclase in $M_{A2M\text{-site}}$ at Asa at the expense
465 of epidote and amphibole (Casetou-Gustafson et al., 2018) was directly reflected in the significant discrepancy
466 and overestimated weathering rates of Ca by $W_{A2M\text{-site}}$ compared to W_{XRPD} (Fig. 5, and 1a). This discrepancy was
467 due to differences between $W_{A2M\text{-site}}$ and W_{XRPD} in the mineral stoichiometry of calcic plagioclases, and not in
468 geochemistry, as the same geochemical analyses were also used for $W_{A2M\text{-reg}}$.
469

470 At Flakaliden, A2M based on site-specific mineralogy overestimated epidote at the expense of amphibole
471 (Casetou-Gustafson et al., 2018), leading to an underestimation of Ca weathering rates from amphibole compared
472 to epidote (Fig. 5). On the other hand, at Asa, it was the regional mineralogy input to A2M that resulted in
473 overestimated amounts of epidote at the expense of dioctahedral vermiculite and amphibole, and this bias was
474 directly reflected in the underestimated release of Ca from amphibole in $W_{A2M\text{-reg}}$. Conversely, the relatively small
475 and non-significant discrepancies of Ca release by $W_{A2M\text{-site}}$ at Flakaliden and by $W_{A2M\text{-reg}}$ at Asa did not depend
476 on a high precision in estimating the contribution from different minerals, since the precision was actually low. In
477 these cases, the good fits seem to be simply coincidental. Owing to differences in dissolution rates, Ca-bearing
478 minerals tend to compensate each other in terms of the total weathering rate that is calculated. This compensatory



479 effect is perhaps the reason why by coincidence, both $W_{A2M-reg}$ and $W_{A2M-site}$ discrepancies for Ca diverge in
480 different directions at Asa compared to Flakaliden.

481

482 Another source of uncertainty associated with the release of Ca is the role of minerals with high dissolution rates
483 that occur in low abundance, for example apatite and pyroxene. Apatite was included in M_{A2M} , but if present in the
484 soils studied was below the detection limit of 1 wt.% in the XRPD analyses (Casetou-Gustafson et al., 2018).
485 Additionally, the assumption made in the A2M calculations that all P determined in the geochemical analyses is
486 allocated to apatite will likely overestimate the abundance of this mineral since soil P can also occur bound to Fe
487 and Al oxides and soil organic matter in acidic mineral soils (Weil and Brady, 2016). The high occurrence of
488 paracrystalline Fe-oxyhydroxide and Al-containing allophane and imogolite at Flakaliden indicates that this could
489 be the case, at least at Flakaliden.

490

491 Regarding pyroxene, XRPD might have failed to detect and quantify pyroxene due to their low abundances at
492 Flakaliden (Casetou-Gustafson et al., 2018). Analytical limitations of XRPD would thus imply that W_{XRPD} of Ca
493 might be underestimated at Flakaliden and Asa. However, in the absence of XRPD detection it is also possible that
494 $M_{A2M-reg}$ overestimated the pyroxene contents at Flakaliden. Thus, apatite and pyroxene added relatively large
495 uncertainties to the weathering estimates of Ca at Flakaliden due to the fact that they have a low abundance in
496 combination with very high dissolution rates. Furthermore, the overestimation of the slowly weatherable mineral
497 illite by $M_{A2M-reg}$ (Casetou-Gustafson et al., 2018) resulted in an underestimation of Ca release by $W_{A2M-reg}$ at
498 Flakaliden, since less Ca was allocated to the more weatherable minerals. Although, it should also be noted
499 parenthetically that Ca can only occur as an exchangeable cation in illite, it is not an element that occurs as part of
500 the illite structure, such that the ‘illite’ composition used in PROFILE may need some revision.

501 **4.3.3 Magnesium release rates**

502 At both study sites, a large number of Mg-containing minerals contributed to the release of Mg, but amphibole
503 was the predominant mineral according to W_{XRPD} and $W_{A2M-site}$. The only significant discrepancy in Mg release
504 rates was revealed for $W_{A2M-site}$ at Asa, which resulted in an overestimation by 41 %. This overestimation was an
505 effect of underestimated contribution from amphibole in combination with overestimated contributions from
506 hydrobiotite and trioctahedral mica. This result for Asa supported our second hypothesis. At Flakaliden, $W_{A2M-site}$
507 produced the same shift in the contribution of Mg by minerals, but the net effect was a very small and non-
508 significant discrepancy to W_{XRPD} . As was noted for Ca, the different outcomes of using site-specific mineralogies
509 at Asa and Flakaliden has no systematic underlying pattern.

510 Using PROFILE based on regional mineralogy resulted in surprisingly low and non-significant discrepancies in
511 Mg release rate, despite both the qualitative and quantitative mineralogies being very different from XRPD,
512 particularly at Flakaliden. For example, both pyroxene and illite were included in $M_{A2M-reg}$, but not in M_{XRPD} . Thus,
513 at Flakaliden, the overestimation of illite in $M_{A2M-reg}$ caused an underestimation of Mg release rates comparable to
514 the underestimation of Ca release rates.



515 4.3.4 Potassium release rates

516 Weathering of K-feldspar was the most important source of K release by PROFILE regardless of the different
517 types of mineralogy input. Casetou-Gustafson et al. (2018) showed a strong negative correlation between $M_{A2M-reg}$
518 and M_{XRPD} for two of the major K-bearing minerals observed at both study sites, i.e., illite and K-feldspar. Contrary
519 to our second hypothesis, the results of the present study demonstrate that over- or underestimation of $W_{A2M-reg}$
520 compared to W_{XRPD} cannot be explained by significant negative correlation of illite and K-feldspar in $M_{A2M-reg}$.
521 However, this is likely related to the fact that illite and K-feldspar have the lowest and also quite similar dissolution
522 rates among minerals included in PROFILE (i.e. the highest dissolution coefficients, Table 3). Although very
523 different inputs in relation to K bearing minerals produced very similar outputs, we note that this appears
524 contradictory to differences in the behaviour of K-feldspars and K-micas as sources of K via weathering to plants
525 as reviewed for example by Thompson and Ukrainczyk (2002).

526 5. Concluding remarks

- 527 • Based on comparing the full solution span of normative mineralogy from the A2M program to measured
528 reference mineralogy from XRPD overall similar weathering rates were generated by the different
529 mineralogical inputs to the PROFILE model. However, the underlying contributions from different
530 minerals to the overall rates differed markedly. Although the similarity of overall rates lends some support
531 to the use of normative mineralogy as input to weathering models, the details of the comparison reveal
532 potential short-comings and room for improvements in the use of normative mineralogies.
- 533 • Compared with regional mineralogy, weathering rates based on site-specific mineralogy were more
534 comparable to the reference rates generated from XRPD mineralogy, in line with hypothesis 1, at one of
535 the study sites (Flakaliden), but not at the other (Asa). Thus, although intuitively the more detailed site
536 specific quantitative mineralogy data might be expected to give more comparable results, this is not
537 supported by this study.
- 538 • For Ca and Mg the differences between weathering rates based on different mineralogies could be
539 explained by differences in the content of some specific Ca- and Mg-bearing minerals, e.g. amphibole,
540 apatite, pyroxene and illite. Improving the precision in the content and presence versus absence of some
541 of these minerals would reduce weathering uncertainties.
- 542 • High uncertainties in mineralogy, due for example to different A2M assumptions, had surprisingly low
543 effect on the weathering from Na- and K-bearing minerals. This can be explained by the fact that the
544 weathering rate constants for the minerals involved, e.g. the plagioclase feldspars and K-feldspar and
545 dioctahedral micas, are similar in PROFILE such that they compensate each other in the overall
546 weathering rate outputs for these elements, a situation that is unlikely to reflect reality.
- 547 • For more in-depth analysis of the uncertainties in weathering rates caused by mineralogy, the rate
548 coefficients of minerals should be revisited and their uncertainties assessed. A revision of rate constants
549 could lead to results more in line with hypothesis 1.

550

551 6. Authors contribution

552 Authors contributed to the study as in the following: S. Casetou-Gustafson: study design, data treatment, PROFILE
553 model analyses, interpretation and writing. C. Akselsson: study design, PROFILE model development,



554 interpretation and writing. B.A. Olsson: study design, interpretation and writing. S. Hillier: interpretation and
555 writing.

556 7. Acknowledgements

557 Financial support from The Swedish research Council for Environment, Agricultural Sciences and Spatial Planning
558 (212-2011-1691) (FORMAS) (Strong Research Environment, QWARTS) and the Swedish Energy Agency
559 (p36151-1). Stephen Hillier acknowledges support of the Scottish Government's Rural and Environment Science
560 and Analytical Services Division (RESAS). We thank Salim Belyazid for his contribution to the design of the
561 study.

562 8. References

563 Aagaard, P., and Helgeson, H. C.: Thermodynamic and kinetic constraints on reaction rates among minerals and
564 aqueous solutions: I. Theoretical considerations, *Am. J. Sci.*, 282, 237-285, 10.2475/ajs.282.3.237, 1982.

565 Akselsson, C., Westling, O., Sverdrup, H., and Gundersen, P.: Nutrient and carbon budgets in forest soils as
566 decision support in sustainable forest management, *Forest Ecol Manag*, 238, 167-174, 2007a.

567 Akselsson, C., Westling, O., Sverdrup, H., Holmqvist, J., Thelin, G., Uggla, E., and Malm, G.: Impact of harvest
568 intensity on long-term base cation budgets in Swedish forest soils, *Water, Air, & Soil Pollution: Focus*, 7, 201-
569 210, 2007b.

570 Akselsson, C., Olsson, J., Belyazid, S., and Capell, R.: Can increased weathering rates due to future warming
571 compensate for base cation losses following whole-tree harvesting in spruce forests?, *Biogeochemistry*, 128, 89-
572 105, 2016.

573 Albaugh, T. J., Bergh, J., Lundmark, T., Nilsson, U., Stape, J. L., Allen, H. L., and Linder, S.: Do biological
574 expansion factors adequately estimate stand-scale aboveground component biomass for Norway spruce? *Forest*
575 *Ecol Manag*, 258, 2628-2637, 2009.

576 Allen, B. L., and Hajek, B. F.: Mineral occurrence in soil environments, in: *Minerals in Soil Environments*, edited
577 by: Dixon, J. B., and Weed, S. B., Soil Science Society of America Inc., Madison, no. 1, 199-278, 1989.

578 Andrist-Rangel, Y., Simonsson, M., Andersson, S., Öborn, I., and Hillier, S.: Mineralogical budgeting of
579 potassium in soil: a basis for understanding standard measures of reserve potassium, *Journal of plant nutrition and*
580 *soil science*, 169, 605-615, 2006.

581 Bergh, J., Linder, S., Lundmark, T., and Elfving, B.: The effect of water and nutrient availability on the
582 productivity of Norway spruce in northern and southern Sweden, *Forest Ecol Manag*, 119, 51-62, 10.1016/s0378-
583 1127(98)00509-x, 1999.

584 Blum, A. E., and Stillings, L. L.: Feldspar dissolution kinetics, in: *Chemical Weathering Rates of Silicate Minerals*,
585 edited by: White, A. F., and Brantley, S. L., *Reviews in Mineralogy, Mineralogical Soc Amer*, Chantilly, 291-351,
586 1995.



587 Casetou-Gustafson, S., Hillier, S., Akselsson, C., Simonsson, M., Stendahl, J., and Olsson, B. A.: Comparison of
588 measured (XRPD) and modeled (A2M) soil mineralogies: A study of some Swedish forest soils in the context of
589 weathering rate predictions, *Geoderma*, 310, 77-88, 2018.

590 Chou, L., and Wollast, R.: Steady-state kinetics and dissolution mechanisms of albite, *Am. J. Sci.*, 285, 963-993,
591 10.2475/ajs.285.10.963, 1985.

592 de Jong, J., Akselsson, C., Egnell, G., Löfgren, S., and Olsson, B. A.: Realizing the energy potential of forest
593 biomass in Sweden—How much is environmentally sustainable?, *Forest Ecol Manag*, 383, 3-16, 2017.

594 Froberg, M., Grip, H., Tipping, E., Svensson, M., Stromgren, M., and Kleja, D. B.: Long-term effects of
595 experimental fertilization and soil warming on dissolved organic matter leaching from a spruce forest in Northern
596 Sweden, *Geoderma*, 200, 172-179, 10.1016/j.geoderma.2013.02.002, 2013.

597 Futter, M. N., Klaminder, J., Lucas, R. W., Laudon, H., and Kohler, S. J.: Uncertainty in silicate mineral
598 weathering rate estimates: source partitioning and policy implications, *Environ Res Lett*, 7, Artn 024025
599 10.1088/1748-9326/7/2/024025, 2012.

600 Hellsten, S., Helmisaari, H. S., Melin, Y., Skovsgaard, J. P., Kaakinen, S., Kukkola, M., Saarsalmi, A., Petersson,
601 H., and Akselsson, C.: Nutrient concentrations in stumps and coarse roots of Norway spruce, Scots pine and silver
602 birch in Sweden, Finland and Denmark, *Forest Ecol Manag*, 290, 40-48, 10.1016/j.foreco.2012.09.017, 2013.

603 Hillier, S.: Use of an air brush to spray dry samples for X-ray powder diffraction, *Clay Miner*, 34, 127-127, 1999.

604 Hillier, S.: Quantitative analysis of clay and other minerals in sandstones by X-ray powder diffraction (XRPD),
605 Clay mineral cements in sandstones, 34, 213-251, 2003.

606 Hodson, M. E., Langan, S. J., and Wilson, M. J.: A sensitivity analysis of the PROFILE model in relation to the
607 calculation of soil weathering rates, *Appl Geochem*, 11, 835-844, Doi 10.1016/S0883-2927(96)00048-0, 1996.

608 Jönsson, C., Warfvinge, P., and Sverdrup, H.: Uncertainty in predicting weathering rate and environmental stress
609 factors with the PROFILE model, *Water, Air, and Soil Pollution*, 81, 1-23, 1995.

610 Karlsson, P.-E., Ferm, M., Hultberg, H., Hellsten, S., Akselsson, C., and Karlsson, G. P.: Totaldeposition av kväve
611 till skog, IVL Swedish Environmental Research Institute, Stockholm, Sweden 37, 2012.

612 Karlsson, P.-E., Ferm, M., Hultberg, H., Hellsten, S., Akselsson, C., and Karlsson, G. P.: Totaldeposition av
613 baskatjoner till skog, IVL Swedish Environmental Research Institute, Stockholm, Sweden 65, 2013.

614 Kleeberg, R.: Results of the second Reynolds Cup contest in quantitative mineral analysis, *International Union of
615 Crystallography. Commission on Powder Diffraction Newsletter*, 30, 22-24, 2005.

616 Kolka, R. K., Grigal, D., and Nater, E.: Forest soil mineral weathering rates: use of multiple approaches,
617 *Geoderma*, 73, 1-21, 1996.



619 Koseva, I. S., Watmough, S. A., and Aherne, J.: Estimating base cation weathering rates in Canadian forest soils
620 using a simple texture-based model, *Biogeochemistry*, 101, 183-196, 10.1007/s10533-010-9506-6, 2010.

621 Kronnäs, V., Akselsson, C., and Belyazid, S.: Dynamic modelling of weathering rates – Is there any benefit over
622 steady-state modelling? *SOIL*, 2019.

623 Langan, S. J., Sverdrup, H. U., and Coull, M.: The calculation of base cation release from the chemical weathering
624 of Scottish soils using the PROFILE model, *Water, air, and soil pollution*, 85, 2497-2502, 1995.

625 Linder, S.: Foliar analysis for detecting and correcting nutrient imbalances in Norway spruce, *Ecological Bulletins*,
626 178-190, 1995.

627 Lofgren, S., Aastrup, M., Bringmark, L., Hultberg, H., Lewin-Pihlblad, L., Lundin, L., Karlsson, G. P., and
628 Thunholm, B.: Recovery of Soil Water, Groundwater, and Streamwater From Acidification at the Swedish
629 Integrated Monitoring Catchments, *Ambio*, 40, 836-856, 10.1007/s13280-011-0207-8, 2011.

630 McCarty, D. K.: Quantitative mineral analysis of clay-bearing mixtures: the “Reynolds Cup” contest, *IUCr CPD*
631 Newsletter, 27, 12-16, 2002.

632 Olsson, M., Rosén, K., and Melkerud, P.-A.: Regional modelling of base cation losses from Swedish forest soils
633 due to whole-tree harvesting, *Appl Geochem*, 8, 189-194, 1993.

634 Omotoso, O., McCarty, D. K., Hillier, S., and Kleeberg, R.: Some successful approaches to quantitative mineral
635 analysis as revealed by the 3rd Reynolds Cup contest, *Clay Clay Miner*, 54, 748-760, 2006.

636 Posch, M., and Kurz, D.: A2M - A program to compute all possible mineral modes from geochemical analyses,
637 *Comput Geosci*, 33, 563-572, 10.1016/j.cageo.2006.08.007, 2007.

638 R, C. T.: R: A Language and Environment for Statistical Computing. R Foundation for Statistical Computing,
639 Vienna, Austria, 2016.

640 Raven, M. D., and Self, P. G.: Outcomes of 12 years of the Reynolds Cup quantitative mineral analysis round
641 robin, *Clay Clay Miner*, 65, 122-134, 2017.

642 Röser, D., Asikainen, A., Raulund-Rasmussen, K., and Møller, I.: Sustainable use of wood for energy—a synthesis
643 with focus on the Nordic–Baltic region. Springer, Berlin, 2008.

644 Simonsson, M., and Berggren, D.: Aluminium solubility related to secondary solid phases in upper B horizons
645 with spodic characteristics, *Eur J Soil Sci*, 49, 317-326, 1998.

646 Staelens, J., Houle, D., De Schrijver, A., Neirynck, J., and Verheyen, K.: Calculating dry deposition and canopy
647 exchange with the canopy budget model: Review of assumptions and application to two deciduous forests, *Water*
648 *Air Soil Poll*, 191, 149-169, 10.1007/s11270-008-9614-2, 2008.

649 Starr, M., Lindroos, A.-J., Tarvainen, T., and Tanskanen, H.: Weathering rates in the Hietajärvi Integrated
650 Monitoring catchment, 1998.



651 Stendahl, J., Lundin, L., and Nilsson, T.: The stone and boulder content of Swedish forest soils, *Catena*, 77, 285-
652 291, 2009.

653 Stendahl, J., Akselsson, C., Melkerud, P.-A., and Belyazid, S.: Pedon-scale silicate weathering: comparison of the
654 PROFILE model and the depletion method at 16 forest sites in Sweden, *Geoderma*, 211, 65-74, 2013.

655 Sverdrup, H., and Warfvinge, P.: Calculating Field Weathering Rates Using a Mechanistic Geochemical Model
656 Profile, *Appl Geochem*, 8, 273-283, Doi 10.1016/0883-2927(93)90042-F, 1993.

657 Sverdrup, H.: Geochemistry, the key to understanding environmental chemistry, *Sci Total Environ*, 183, 67-87,
658 1996.

659 Sverdrup, H., and Rosen, K.: Long-term base cation mass balances for Swedish forests and the concept of
660 sustainability, *Forest Ecol Manag*, 110, 221-236, 1998.

661 Thompson, M. L., and Ukrainezyk, L.: Micas, Soil mineralogy with environmental applications, edited by: Dixon,
662 J. B., and Schulze, D. G., Soil Science Society of America Inc., Madison, 431-466 pp., 2002.

663 Warfvinge, P., and Sverdrup, H.: Critical loads of acidity to Swedish forest soils: methods, data and results, Lund
664 University, 1995.

665 Weil, R. R., and Brady, N. C.: Soil phosphorus and potassium, in: The nature and properties of soils, Ed. 15,
666 Pearson Education, Upper Saddle River, USA, 2016.

667 Whitfield, C., Watmough, S., Aherne, J., and Dillon, P.: A comparison of weathering rates for acid-sensitive
668 catchments in Nova Scotia, Canada and their impact on critical load calculations, *Geoderma*, 136, 899-911, 2006.

669 Wikstrom, P., Edenuis, L., Elfving, B., Eriksson, L. O., Lamas, T., Sonesson, J., Ohman, K., Wallerman, J., Waller,
670 C., and Klintebäck, F.: The Heureka forestry decision support system: an overview, *Mathematical and
671 Computational Forestry and Natural Resources Sciences*, 3, 87-94, 2011.

672 Viro, P. J.: On the determination of stoniness, *Communicationes Instituti Forestalis Fenniae*, 40, 23, 1952.

673 Yu, L., Belyazid, S., Akselsson, C., van der Heijden, G., and Zanchi, G.: Storm disturbances in a swedish forest—
674 A case study comparing monitoring and modelling, *Ecol Model*, 320, 102-113, 2016.

675 Yu, L., Zanchi, G., Akselsson, C., Wallander, H., and Belyazid, S.: Modeling the forest phosphorus nutrition in a
676 southwestern Swedish forest site, *Ecol Model*, 369, 88-100, 2018.

677 Zanchi, G., Belyazid, S., Akselsson, C., and Yu, L.: Modelling the effects of management intensification on
678 multiple forest services: a Swedish case study, *Ecol Model*, 284, 48-59, 2014.

679 Zetterberg, T., Kohler, S. J., and Lofgren, S.: Sensitivity analyses of MAGIC modelled predictions of future
680 impacts of whole-tree harvest on soil calcium supply and stream acid neutralizing capacity, *Sci Total Environ*,
681 494, 187-201, 10.1016/j.scitotenv.2014.06.114, 2014.



687 **Table 1.** Characteristics of the study sites.

Site	Asa	Flakaliden
Coordinates ^a	57° 08' N; 14° 45' E	64° 07' N; 19° 27' E
Elevation (m a.s.l.) ^a	225-250	310-320
Mean annual precipitation (mm) ^b	688	523
Mean annual air temperature (°C) ^b	5.5	1.2
Bedrock ^c	Acidic intrusive rock	Quartz-feldspar-rich sedimentary rock
Soil texture ^d	Sandy loam	Sandy loam
Type of quaternary deposit ^d	Sandy loamy till	Sandy loamy till
Soil moisture regime (Soil taxonomy) ^e	Udic	Udic
Soil type (USDA soil taxonomy) ^e	Spodosols	Spodosols
Region/province ^f	3	1

^a Bergh et al. 2005

^b Long-term averages of annual precipitation and temperature data (1961-1990) from nearest SMHI meteorological stations (Asa: Berg; Flakaliden: Kullbäcksliden)

^c SGU bedrock map (1:50000)

^d Soil texture based on own particle size distribution analysis by wet sieving according to ISO 11277

^e USDA Soil Conservation service, 2014

^f Warfvinge and Sverdrup (1995)



689 **Table 2.** PROFILE parameter description.

Parameter	Description	Unit	Source
Temperature	Site	°C	Measurements from nearby SMHI stations
Precipitation	Site	m yr	Measurements from nearby SMHI stations
Total deposition	Site	mmol _c m ⁻² yr ⁻¹	Measurements of open field and throughfall deposition available from nearby Swedish ICP Integrated Monitoring Sites
BC net uptake	Site	mmol _c m ⁻² yr ⁻¹	Previously measured data from Asa and Flakaliden: Element concentration in biomass from Linder (unpublished data). Biomass data from Heureka simulations.
N net uptake	Site	mmol _c m ⁻² yr ⁻¹	Previously measured data from Asa and Flakaliden: Element concentration in biomass from Linder (unpublished data). Biomass data from Heureka simulations.
BC in litterfall	Site	mmol _c m ⁻² yr ⁻¹	Literature data for element concentrations from Hellsten et al. 2013
N in litterfall	Site	mmol _c m ⁻² yr ⁻¹	Literature data for element concentrations from Hellsten et al. 2013
Evapofraction	Site	Fraction	Own measurements and measurements from nearby Swedish Integrated Monitoring Sites
Mineral surface area	Soil	m ² m ⁻³	Own measurements used together with Eq. 5.13 in Warfvinge and Sverdrup (1995)
Soil bulk density	Soil	kg m ⁻³	Own measurements
Soil moisture	Soil	m ³ m ⁻³	Based on paragraph 5.9.5 in Warfvinge and Sverdrup (1995)
Mineral composition	Soil	Weight fraction	Own measurements
Dissolved organic carbon	Soil	mg l ⁻¹	Previously measured data from Asa and Flakaliden: Measurements for B-horizon from Harald Grip and previously measured data from Fröberg et al. 2013
Aluminium solubility coefficient	Soil	kmol m ⁻³	Own measurements for total organic carbon and oxalate extractable aluminium together with function developed from previously published data (Simonsson and Berggren, 1998)
Soil solution CO ₂ partial pressure	Soil	atm.	Base on paragraph 5.10.2 in Warfvinge and Sverdrup (1995)

690

691



692 **Table 3** Mineral dissolution rate coefficients ($\text{kmol}_c \text{ m}^{-2} \text{ s}^{-1}$) used in PROFILE for the reactions with H^+ , H_2O ,
693 CO_2 and organic ligands (R^+) (Warfvinge and Sverdrup, 1995).

Mineral	pkH	pkH ₂ O	pkCO ₂	pKR
Pyroxene	12.3	17.5	15.8	14.4
Apatite	12.8	15.8	15.8	19.5
Amphibole	13.3	16.3	15.9	14.4
Epidote	14	17.2	16.2	14.4
Plagioclase	14.6	16.8	15.9	14.7
K-Feldspar	14.7	17.2	16.8	15
Biotite	14.8	16.7	15.8	14.8
Chlorite	14.8	17	16.2	15
Vermiculite	14.8	17.2	16.2	15.2
Muscovite and Illite	15.2	17.5	16.5	15.3

694

695

696

697

698

699

700

701

702

703

704

705

706

707

708

709

710



711 **Figure captions**

712 **Figure 1.** The first scenario for describing the effect of mineralogy on weathering rates in the upper mineral soil
713 for a specific soil profile (a) happens when the PROFILE weathering rate based on XRPD (reference weathering
714 rates) is not contained in the weathering range produced using PROFILE in combination with the full A2M
715 solution space. There are two possible explanations of why a significant discrepancy introduces an uncertainty
716 range, i.e. (1) due to uncertainties related to the mineralogical A2M input and (2) due to uncertainties related to
717 the limitation of the XRPD method itself (i.e. detection limit). The second scenario (b) occurs when the reference
718 weathering rate is contained in the full A2M weathering span. In this case we speak of 'non-significant
719 discrepancies'.

720 **Figure 2.** Comparison of PROFILE weathering rates of base cations ($\text{mmol}_c \text{ m}^{-2} \text{ yr}^{-1}$) at Asa (a) and Flakaliden
721 (b) sites in the 0–50 cm horizon based on XRPD mineralogy (vertical dashed lines) with PROFILE weathering
722 rates based on one thousand random regional A2M mineralogies versus one thousand random site-specific A2M
723 mineralogies. Data presented are from four different soil profiles per site. Regional graph for soil profile 10B at
724 Flakaliden is missing since A2M did not calculate 1000 solutions for soil layer 20–30, due to "Non-positive
725 solution".

726 **Figure 3.** Root-mean square error (RMSE) of average PROFILE weathering rates ($\text{mmol}_c \text{ m}^{-2} \text{ yr}^{-1}$) of one
727 thousand A2M mineralogies per soil layer, compared to weathering rates based on XRPD mineralogy per soil
728 layer. Comparisons are based on the total weathering per element (A) and on the sum of mineral contributions to
729 total weathering per element (B). RMSE describes the prediction accuracy for a single soil layer.

730 **Figure 4.** Comparison of PROFILE weathering rates based on XRPD mineralogy ($\text{mmol}_c \text{ m}^{-2} \text{ yr}^{-1}$) with
731 PROFILE weathering rates based on regional A2M mineralogy (upper figures) versus site-specific mineralogy
732 (lower figures). Each data point represents a mean of one thousand PROFILE weathering rates for a specific soil
733 depth of one of 4 soil profiles per site.

734 **Figure 5.** Comparison of sums of PROFILE base cation weathering rates for different minerals in the upper
735 mineral soil (0–50 cm) based on XRPD mineralogy and the average PROFILE base cation weathering rate (i.e.
736 based on one thousands input A2M mineralogies per mineral) according to the two normative mineralogical
737 methods and for each study site (i.e. Asa site-specific, Flakaliden site-specific, Asa regional, Flakaliden
738 regional). For W_{A2M} , relative error (% of W_{XRPD} estimate) are given at the end of each bar to illustrate the
739 average deviation of W_{A2M} and W_{XRPD} in the upper mineral soil. *=significant discrepancy as defined in section
740 2.7. Vrm1=Trioctahedral vermiculite; Vrm2=Diocahedral vermiculite. Information on chemical compositions of
741 minerals are given in Table S5 and S6.

742 **Figure 6.** Sum of weathering rates ($\text{mmol}_c \text{ m}^{-2} \text{ year}^{-1}$) in the upper mineral soil (0–50 cm) for Ca, Mg, K and Na
743 for Asa (A) and Flakaliden (B) and for nearby sites from Stendahl et al. (2013) (Bodafors, Lammhult,
744 Svartholmen and Vindeln).

745

746

747

748

749

750

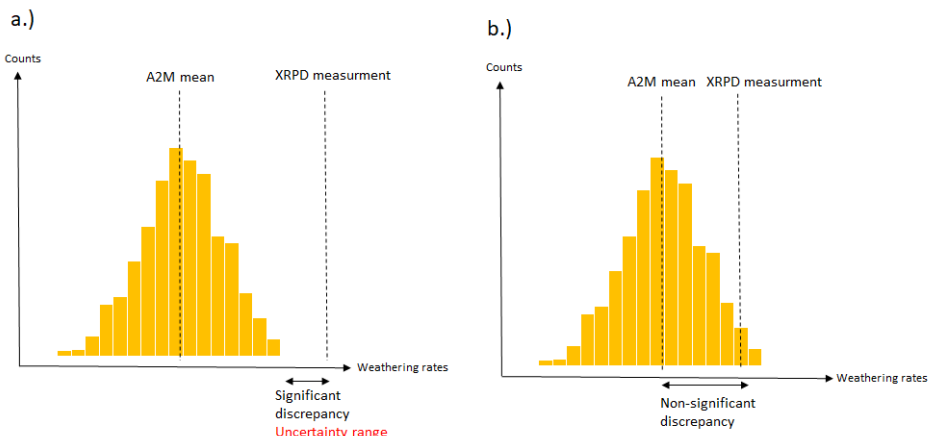
751

752



753

754



755

756 Figure 1a,b

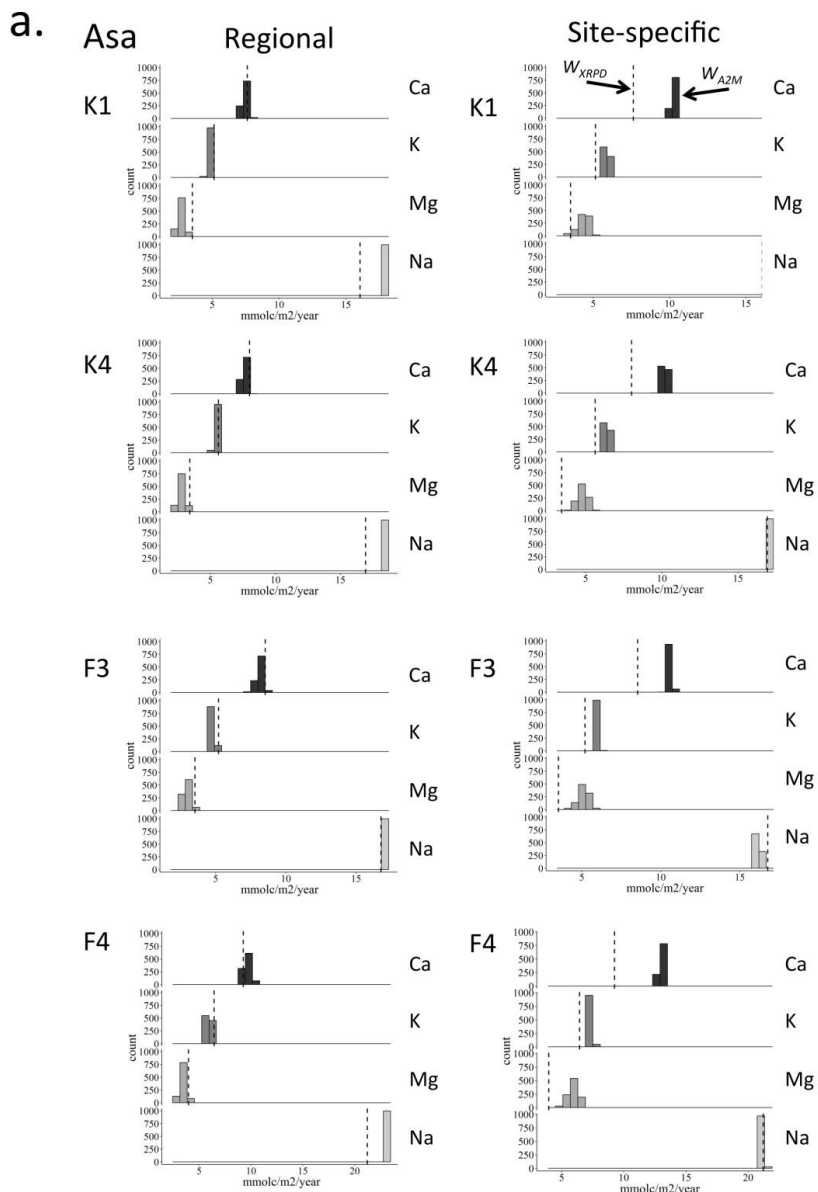
757

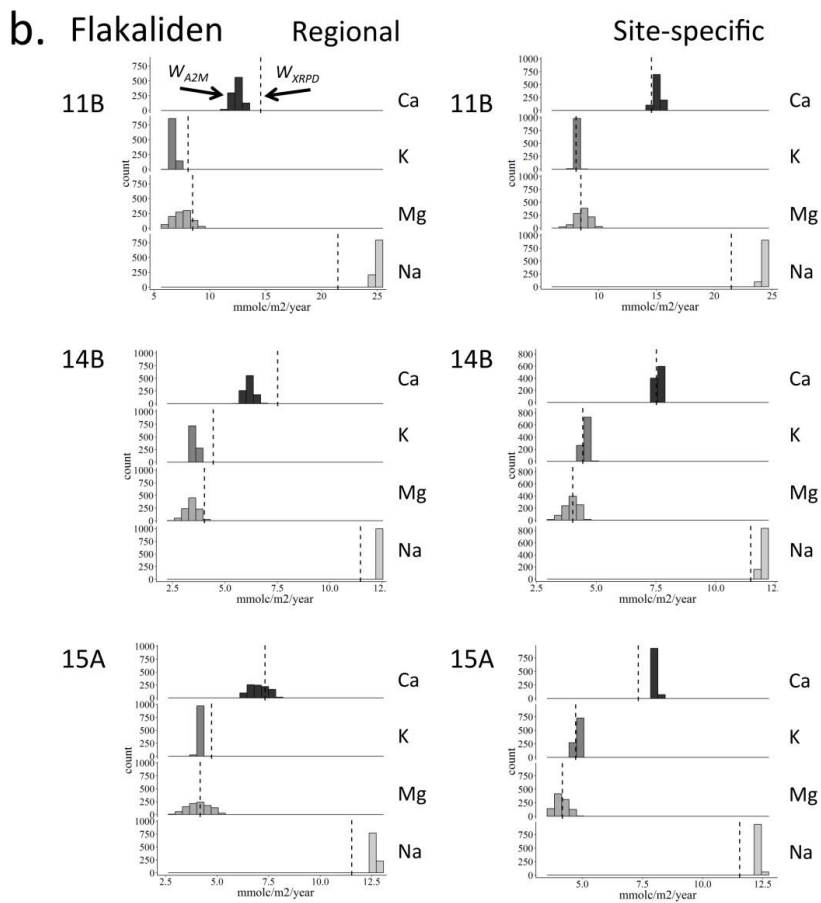
758

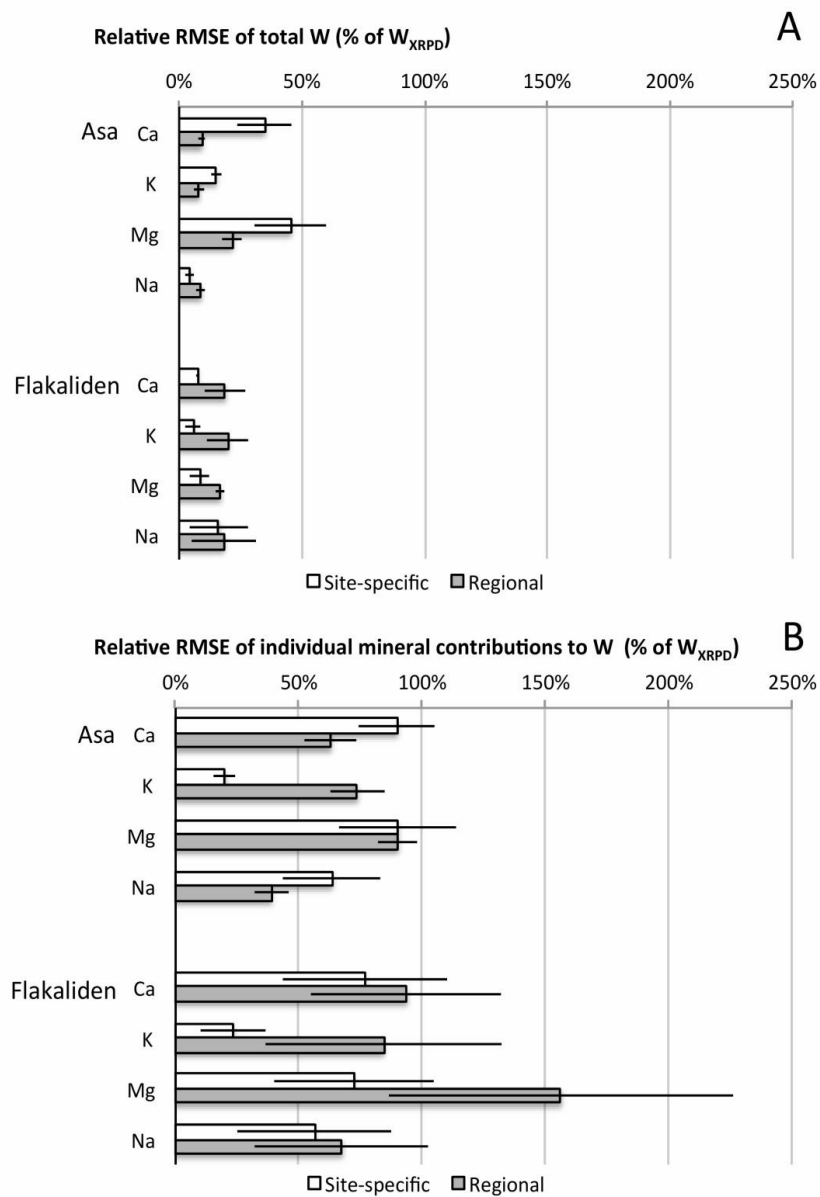
759

760

761







766

767 Figure 3, A, B

768

769

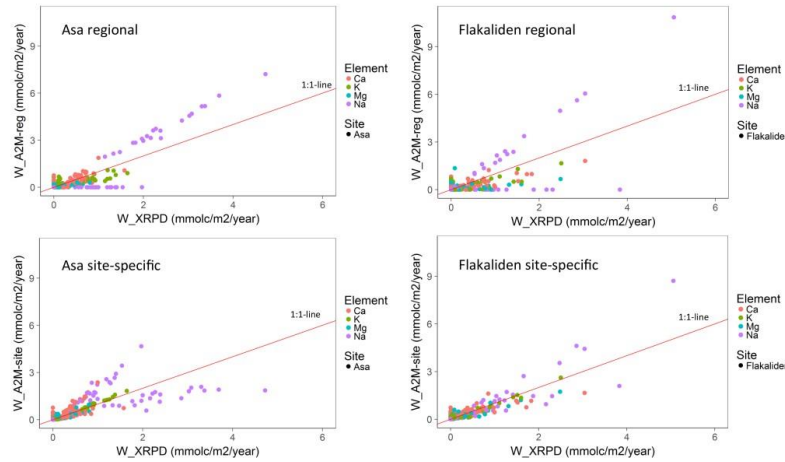
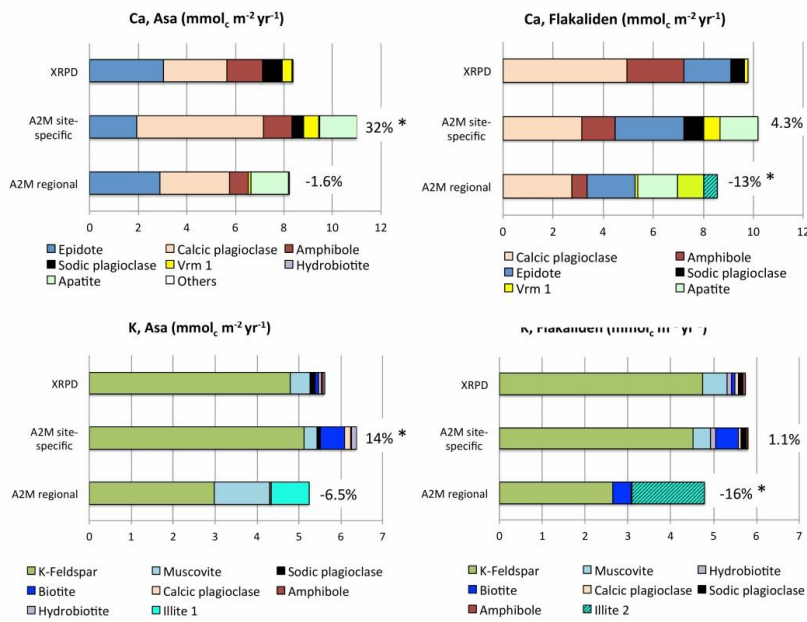


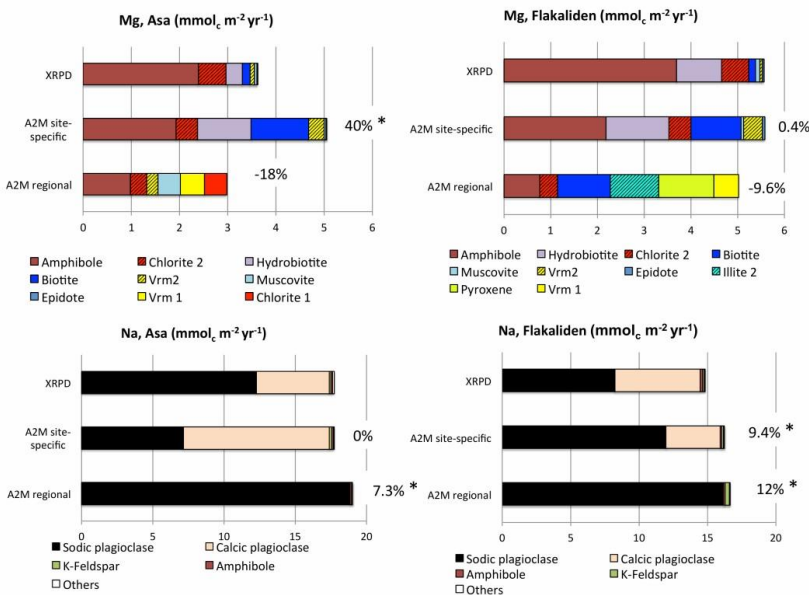
Figure 4



770



773



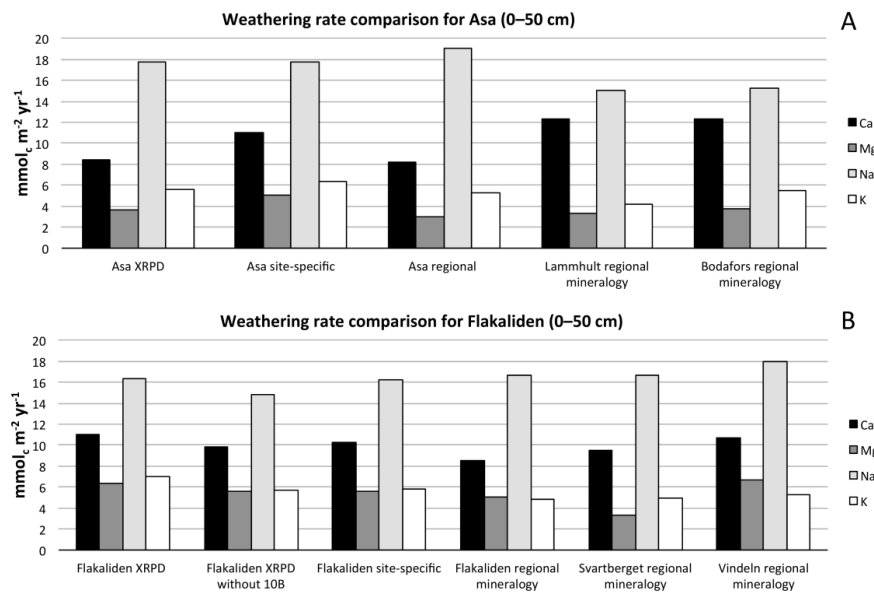
774

775 Figure 5

776



777



778

779 Figure 6 a, b